



SC-FDE for MMF short reach optical interconnects using directly modulated 850 nm VCSELs

Teichmann, Victor S. C.; Barreto, Andre N.; Pham, Tien Thang; Rodes Lopez, Roberto; Tafur Monroy, Idelfonso ; Mello, Darli A. A.

Published in:
Optics Express

Link to article, DOI:
[10.1364/OE.20.025369](https://doi.org/10.1364/OE.20.025369)

Publication date:
2012

Document Version
Publisher's PDF, also known as Version of record

[Link back to DTU Orbit](#)

Citation (APA):
Teichmann, V. S. C., Barreto, A. N., Pham, T. T., Rodes Lopez, R., Tafur Monroy, I., & Mello, D. A. A. (2012). SC-FDE for MMF short reach optical interconnects using directly modulated 850 nm VCSELs. *Optics Express*, 20(23), 25369-25377. <https://doi.org/10.1364/OE.20.025369>

General rights

Copyright and moral rights for the publications made accessible in the public portal are retained by the authors and/or other copyright owners and it is a condition of accessing publications that users recognise and abide by the legal requirements associated with these rights.

- Users may download and print one copy of any publication from the public portal for the purpose of private study or research.
- You may not further distribute the material or use it for any profit-making activity or commercial gain
- You may freely distribute the URL identifying the publication in the public portal

If you believe that this document breaches copyright please contact us providing details, and we will remove access to the work immediately and investigate your claim.

SC-FDE for MMF short reach optical interconnects using directly modulated 850 nm VCSELs

Victor S. C. Teichmann,¹ Andre N. Barreto,¹ Tien-Thang Pham,²
Roberto Rodes,² Idelfonso T. Monroy,² and Darli A. A. Mello^{1,*}

¹OCNLab, Department of Electrical Engineering, University of Brasilia, Brazil

²DTU Fotonik, Department of Photonics Engineering, Technical University of Denmark,
Denmark

*darli@umb.br

Abstract: We propose the use of single-carrier frequency-domain equalization (SC-FDE) for the compensation of modal dispersion in short distance optical links using multimode fibers and 850 nm VCSELs. By post-processing of experimental data, we demonstrate, at 7.9% overhead, the error-free transmission (over a 4 Mbit sequence) of OOK-modulated 5 Gbps over 2443 meters of OM3 fiber (with a nominal 3300 MHz×km bandwidth). The proposed solution may be applied as a low cost alternative for data center and supercomputer interconnects.

© 2012 Optical Society of America

OCIS codes: (060.2360) Fiber optics links and subsystems; (060.4510) Optical communications.

References and links

1. A. V. Rylakov, C. L. Schow, F. E. Doany, B. G. Lee, C. Jahnes, Y. Kwark, C. Baks, D. M. Kuchta, and J. A. Kash, "A 24-channel 300 Gb/s 8.2 pJ/bit full-duplex fiber-coupled optical transceiver module based on a single holey CMOS IC," in *Optical Fiber Communication Conference* (Optical Society of America, 2010), pp. 1–3.
2. A. Vahdat, Hong Liu, Xiaoxue Zhao, and C. Johnson, "The emerging optical data center," in *Optical Fiber Communication Conference* (Optical Society of America, 2011), pp. 1–3.
3. L. Aronson and L. Buckman, "Guide to HP Labs ROFL/OFL fiber measurements from 12/15/97–12/19/97 IEEE 802.3 10 GbE Study Group," <http://www.ieee802.org/3/z/mbi/index/html>.
4. L. Raddatz, I. H. White, D. G. Cunningham, and M. C. Nowell, "An experimental and theoretical study of the offset launch technique for the enhancement of the bandwidth of multimode fiber links," *J. Lightwave Technol.* **16**, 324–331 (1998).
5. L. A. Buckman, B. E. Lemoff, A. J. Schmit, R. P. Tella, and W. Gong, "Demonstration of a small-form-factor WWDM transceiver module for 10-Gb/s local area networks," *IEEE Photon. Technol. Lett.* **14**, 702–704 (2002).
6. C. F. Lam, Hong Liu, B. Koley, Xiaoxue Zhao, V. Kamalov, and V. Gill, "Fiber optic communication technologies: what's needed for datacenter network operations," *IEEE Commun. Mag.* **48**, 32–39 (2010).
7. D. J. F. Barros and J. M. Kahn, "Comparison of orthogonal frequency-division multiplexing and on-off keying in direct-detection multimode fiber links," *J. Lightwave Technol.* **29**, 2299–2309 (2011).
8. J. M. Tang, P. M. Lane, and K. A. Shore, "Transmission performance of adaptively modulated optical OFDM signals in multimode fiber links," *IEEE Photon. Technol. Lett.* **18**, 205–207 (2006).
9. X. Q. Jin, J. M. Tang, K. Qiu, and P. S. Spencer, "Statistical investigations of the transmission performance of adaptively modulated optical OFDM signals in multimode fiber links," *J. Lightwave Technol.* **26**, 3216–3224 (2008).
10. Y. Benlachtar, R. Bouziane, R. I. Killey, C. R. Berger, P. Milder, R. Koutsoyannis, J. C. Hoe, M. Pusc, and M. Glick, "Optical OFDM for the data center," in *Proceedings of International Conference on Transparent Optical Networks* (2010), pp. 1–4.
11. J. Armstrong, "OFDM for optical communications," *J. Lightwave Technol.* **27**, 189–204 (2009).
12. N. Benvenuto, and S. Tomasin, "On the comparison between OFDM and single carrier modulation with a DFE using a frequency-domain feedforward filter," *IEEE Trans. Commun.* **50**, 947–955 (2002).

13. A. Gusmao, R. Dinis, J. Conceicao, and N. Esteves, "Comparison of two modulation choices for broadband wireless communications," in *Proceedings of IEEE Vehicular Technology Conference (2000)*, pp. 1300–1305.
 14. A. Czylik, "Comparison between adaptive OFDM and single carrier modulation with frequency domain equalization," in *Proceedings of IEEE Vehicular Technology Conference (1997)*, pp. 865–869.
 15. M. Wolf, L. Grobe, M. R. Rieche, A. Koher, and J. Vucic, "Block transmission with linear frequency domain equalization for dispersive optical channels with direct detection," in *Proceedings of International Conference on Transparent Optical Networks (2010)*, pp. 1–8.
 16. M. Wolf and L. Grobe, "Block transmission with frequency domain equalization in the presence of colored noise," in *Proceedings of International Conference on Transparent Optical Networks (2011)*, pp. 1–4.
 17. D. Falconer, S. L. Ariyavisitkul, A. Benyamin-Seeyar, and B. Eidson, "Frequency domain equalization for single-carrier broadband wireless systems," *IEEE Commun. Mag.* **40**, 58–66 (2002).
-

1. Introduction

Multimode fibers (MMFs) are widespread in short-reach optical systems, with applications ranging from local-area intracampus communications to data center and supercomputer interconnects. The main reason for the remarkable success of MMFs is their relatively large core radius in comparison to single-mode fibers, which simplifies the component-to-fiber alignment and, therefore, reduces the overall system cost. In particular, the capacity demand for data center and supercomputer interconnects has been satisfied by low-cost solutions composed of vertical cavity surface emitting lasers (VCSELs) directly modulated at the wavelength of 850 nm, MMF transmission, and direct detection [1]. The volume of traffic in data center communications is already enormous, and the fraction of Internet traffic which takes place within the data center is increasing [2]. Therefore, new technologies are needed to increase capacity while maintaining footprint and power consumption. One of the main challenges is to cope with a highly variable modal dispersion from fiber to fiber, which causes a large variation of the link bandwidth [3]. Several solutions to the bandwidth variation problem have been proposed, including restricted offset launch [4] and coarse wavelength division multiplexing (CWDM) [5]. Transmission parallelization has been also deployed by the use of ribbon fibers, however, the associated connectors (MPO/MPT) are relatively costly [6]. In the universe of electronic dispersion compensation, pulse-amplitude modulation (PAM) with decision feedback equalizers has been investigated [7]. Recently, optical orthogonal frequency division multiplexing (OFDM) has proved to be an effective solution to the intersymbol interference (ISI) caused by an optical dispersive channel [8–10]. The main disadvantage of OFDM, however, is that it involves the generation of complicated waveforms, requiring a potentially expensive digital-to-analog converter (DAC) at the transceiver. Another problem is the well-known high peak-to-average power ratio (PAPR), which may cause distortions due to the nonlinear nature of the modulator. In addition, intensity modulated signals are not only real, but also unipolar, which requires the use of artifices such as hermitian symmetry, DC-level addition and clipping, thereby reducing the overall system efficiency [11].

In this paper we propose the use of single-carrier frequency-domain equalization (SC-FDE) for the compensation of modal dispersion in short distance optical links using multimode fibers and 850 nm VCSELs. The SC-FDE architecture has clear similarities with OFDM, including frequency domain equalization using FFTs/IFFTs and the insertion of a cyclic prefix. The main difference from traditional OFDM is that the inverse Fourier transform (IDFT) is moved from the transmitter to the receiver. In fact, SC-FDE has received significant attention as an alternative to traditional OFDM for wireless communications, and there are several studies comparing the performance of both techniques [12–14]. For optical wireless links, block transmission with frequency domain equalization has already been investigated [15, 16]. The main advantage of SC-FDE in comparison to OFDM is that the generated waveforms are simple, usually avoiding the need for a digital to analog converter (DAC) at the transmitter, thus reducing the transceiver cost. Another benefit is that it provides an inherent frequency diversity, which is not the case

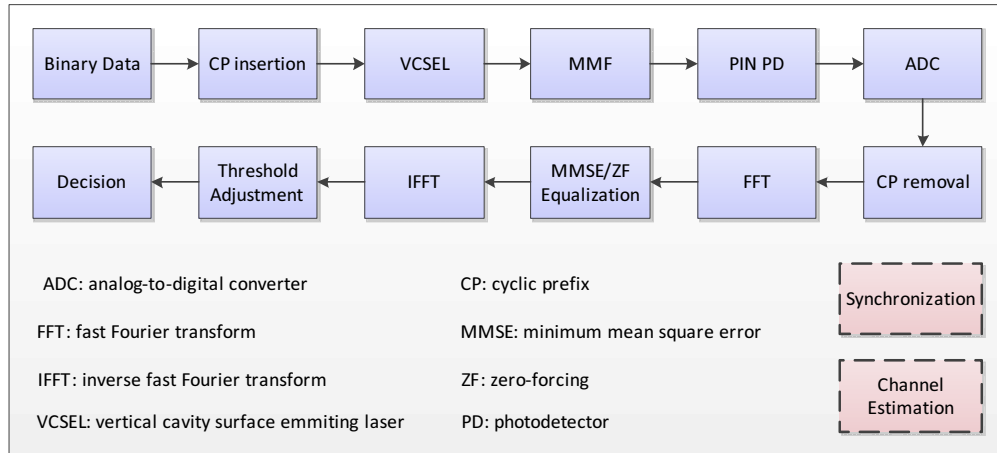


Fig. 1. The SC-FDE block diagram. Upper boxes represent procedures that are made block by block, whereas the side boxes represent procedures performed on pilot blocks only.

in OFDM. In this paper, for example, the transmitter is a simple OOK directly modulated VCSEL, and the receiver analog-to-digital conversion is implemented at the symbol rate. As a drawback, OFDM bit loading is not possible, but it is unlikely that adaptive modulation is used in short-reach systems, given the cost and complexity of the required receiver-transmitter feedback. Finally, when compared to time-domain equalization, frequency-domain equalization is generally more computationally efficient for a sufficiently long channel response (see, for example, Fig. 4 of [17]). With FDE, complexity can be kept within desired bounds by a careful choice of the FFT length, and it is independent of the channel response length. Note, however, that computational efficiency comes at the cost of overhead required by the cyclic prefix.

This paper is organized as follows: Section 2 describes the SC-FDE system, including discussions on channel estimation and frame synchronization. Section 3 presents the experimental results, including a comparison between zero-forcing and minimum mean square error (MMSE) equalization. Lastly, Section 4 concludes the paper.

2. Single-carrier frequency-domain equalization

2.1. Concept

The block diagram of the SC-FDE system is shown in Fig. 1. The concept is very similar to that of OFDM with the difference that, in SC-FDE, the IFFT block is moved from the transmitter to the receiver. Thus, SC-FDE and OFDM have equivalent complexity, although the transmitter in the first case is simpler and the receiver is more complex. At the transmitter, a binary (in this paper, we consider OOK transmission) data sequence of length N_b is generated. This sequence is then split into N_s blocks, and a cyclic prefix (CP) is added to each block, in such a way that the last N_{cp} bits of the block are repeated at the beginning. Each block with cyclic prefix forms a so-called SC-FDE block. Thus, each SC-FDE block has size $S = \frac{N_b}{N_s} + N_{cp}$ bits, and the transmitted sequence \mathbf{X} has size $S \times N_s$. To avoid interblock interference between SC-FDE blocks, the condition $T_{cp} > T_{ch}$ must be satisfied, where $T_{cp} = N_{cp}T_b$ is the temporal duration of the cyclic prefix, T_{ch} is the maximum delay spread of the channel and T_b is the bit duration. Data blocks are alternated with pilot and synchronization blocks, composing a frame of length $S \times N_s + K$, where K is the overhead length, including pilot and frame synchronization sequences. The

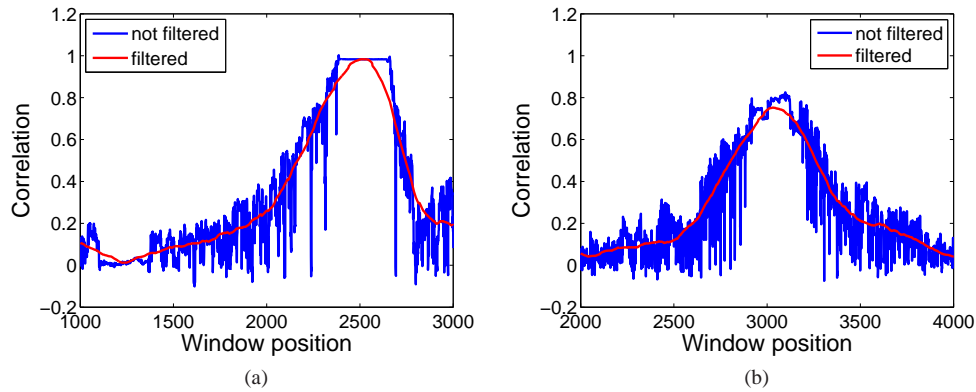


Fig. 2. Correlation between the original and the expected synchronization block versus the window position for (a) back-to-back and (b) fiber transmission.

periodicity of a frame is chosen as to optimize the trade-off between overhead and channel tracking. The SC-FDE blocks are then converted to the analog domain by the modulator (in our case, a directly modulated VCSEL). At the receiver site, the PIN photodetector makes the optical-to-electrical conversion, and the resulting electrical signal is sampled by the analog-to-digital converter, forming sequence \mathbf{Y} .

2.2. Frame synchronization

SC-FDE requires frame synchronization to determine the block position in the received sequence. In this paper, we send a synchronization block along each frame. The synchronization block was chosen among several randomly generated sequences so as to narrow its autocorrelation function. The implemented synchronization algorithm works as follows:

1. Set a non-negative integer n to zero.
2. A window \mathbf{W} of size S bits is taken from the received signal \mathbf{Y} at the positions $Y_n, Y_{n+1} \dots Y_{n+S-1}$.
3. Assuming that this sequence is a pilot sequence, the channel response is estimated (the channel estimation and the equalization process are described below).
4. The S subsequent bits, $Y_{n+S}, Y_{n+S+1} \dots Y_{n+2S-1}$, which should form the synchronization block, are equalized using the channel response estimate calculated in the previous step.
5. The result is correlated with the original synchronization block, resulting in the instant correlation C_n .
6. Increase the value of n by one unit.
7. Repeat $S \times N_s + K - 1$ times steps 2 to 6.

The result of the algorithm is the correlation vector \mathbf{C} of size $S \times N_s + K$. An example of \mathbf{C} is shown in Fig. 2(a) for back-to-back transmission and a data rate of 8 Gbps. In the case without filtering, there are several high correlation points, showing that there is more than one window position that results in optimal detection. This happens because of the redundancy added to the

signal by the cyclic prefix. Thus, there are $M + 1$ possible detection windows, where M is the number of cyclic prefix samples not corrupted by modal dispersion. The algorithm assumes the correct n as the one that leads to the maximum correlation. However, correlation values at the edge of the *plateau* in Fig. 2(a) may also have values close to the optimal, what can lead to synchronization errors. We solve this problem by smoothing \mathbf{C} by a moving average filter of length equal to the cyclic prefix, in such a way that the maximum occurs in the middle of the *plateau*. Figure 2(b) shows the effect of modal dispersion on the correlation vector. Here, the previously mentioned *plateau* is distorted, as most of the cyclic prefix has been corrupted by interblock interference. However, even in the presence of modal dispersion, the frame start is clearly found.

2.3. Equalization

After the synchronization process, the cyclic prefix of each block is removed and the signal is converted to the frequency domain using a FFT. The channel estimator then uses the pilot blocks to estimate the modal dispersion degrading the optical signal. This process is performed whenever a pilot block is received. The channel transfer function is estimated by:

$$H'(f) = \frac{P_o(f)}{P_i(f)}, \quad (1)$$

where $P_o(f)$ and $P_i(f)$ are the Fourier transforms of the received pilot and transmitted pilot blocks, respectively, and $H'(f)$ is the estimate of $H(f)$, the channel transfer function. For a highly dispersive channel like the multimode fiber, frequency-domain equalization becomes attractive. This is true because modal dispersion spreads the transmitted bits in time, which, for high data rates, may cause severe intersymbol interference even for short transmission distances. In this case, time-domain equalization requires generally filters of higher complexity than the frequency-domain counterpart. In this paper we investigated both the MMSE and zero-forcing equalizers. The zero-forcing equalizer frequency response is simply the inverse of the estimated channel transfer function [15]:

$$F_{ZF}(f) = \frac{1}{H'(f)}, \quad (2)$$

and the MMSE equalizer frequency response is calculated by [15]:

$$F_{MMSE}(f) = \frac{H'(f)^*}{|H'(f)|^2 + \text{SNR}^{-1}}, \quad (3)$$

where $(\cdot)^*$ represents the complex conjugate, and SNR is the signal-to-noise ratio at the output of the receiver filter. Once the signal has been equalized, its converted back to the time domain by an IFFT. Before decision, it is necessary to adjust the proper decision threshold.

3. Experimental setup and results

3.1. Experimental setup

A user-defined pattern of 4 Mbits containing pilot, synchronization and data bits was loaded to a pulse pattern generator (PPG). Each frame contains one pilot block of length 1076 bits, followed by one synchronization block of the same length, and 68864 bits of data, already including the cyclic prefixes. The length of the cyclic prefix is 52 bits, and it is added for every 1024 bits. The PPG output drives a commercially available 10 GHz 850 nm VCSEL using a Bias T. The data rate was varied from 5 to 10 Gbps with 0.25 Gbps steps, while the peak-to-peak voltage (V_{p-p}) of the data was fixed at 750 mV. The VCSEL, with a 1 mA threshold current, was biased at

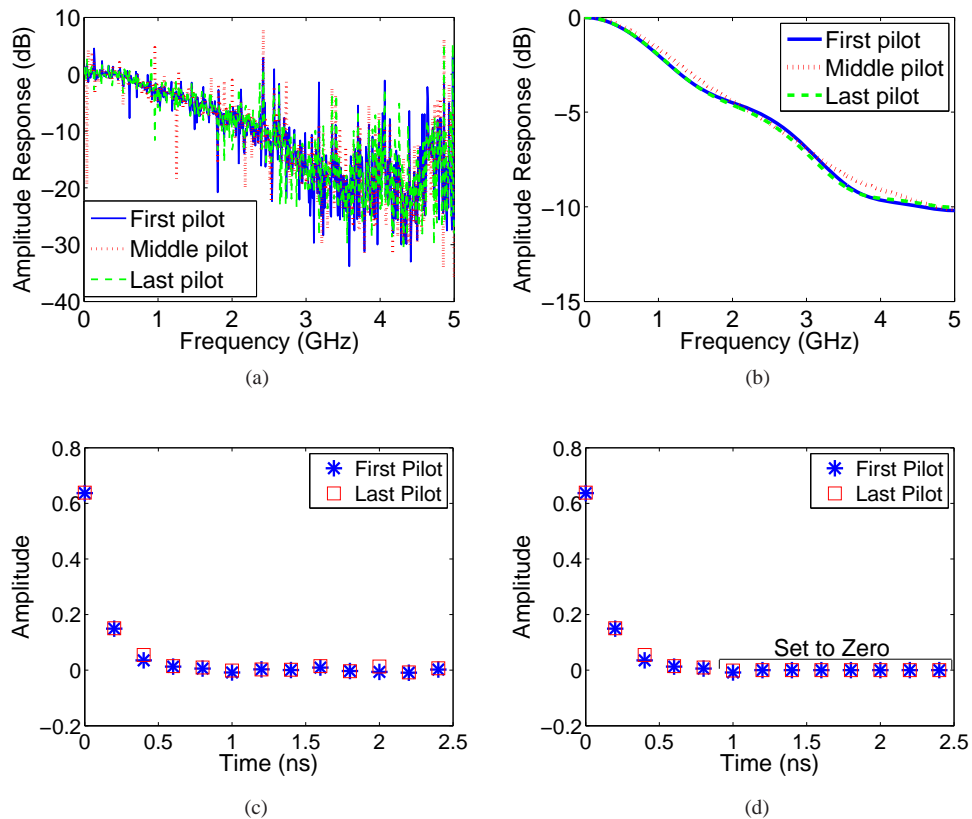


Fig. 3. On the left: channel frequency response (top) and impulse response (bottom) estimations before the impulse response restriction. On the right: channel frequency response (top) and impulse response (bottom) estimations after the impulse response restriction.

6.5 mA for best performance. The root-mean-square (RMS) spectral width of the VCSEL was 0.4 nm. The output optical signal of the VCSEL was transmitted through a 2443 m OM3 MMF with effective modal bandwidth (EMB) of 3300 MHz×km. The optical power before and after fiber transmission was -4.5 and -9.0 dBm, respectively. After fiber transmission, the optical signal was detected by a 10 GHz bandwidth photodetector (PD). The photodetected signal was digitized into a 60 MSample sequence using a 40 GSamples/s digital storage oscilloscope (DSO) for offline digital signal processing (DSP). The stored sequence was first resampled to 4 times the transmission rate, and then was downsampled, keeping one out of every four samples. This process effectively reduced the signal to one sample per bit. The best sample among the available four was chosen as the one that yielded the highest maximum correlation in the frame synchronization process described in Section 2.2. The reception filter was a butterworth filter of 3 dB bandwidth equal to the signal rate.

3.2. Experimental results

Figure 3(a) shows the estimated channel frequency response for a 5 Gbps transmission. The peaks and dips indicate that the estimated frequency response is strongly affected by noise. Thus, some form of smoothing is necessary to have a satisfactory estimate. To reduce the noise

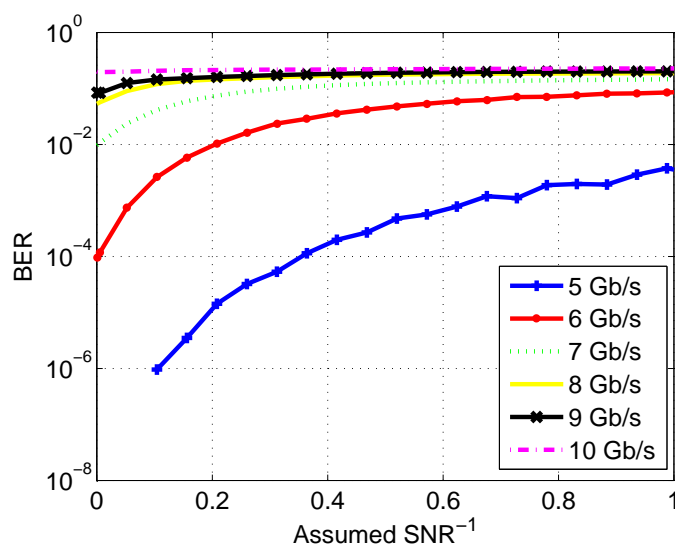


Fig. 4. MMSE equalizer performance. The SNR^{-1} parameter of Eq. (3) was varied from zero to one, and the BER calculated for several transmission rates. The received signal power was kept constant at -9 dBm. An assumed SNR^{-1} equal to zero turns the MMSE equalizer into a zero-forcing equalizer.

impact on the channel estimation, we made an impulse response restriction. This approach is commonly used when the channel impulse response is known to be bounded to a certain duration. This way, we locate the highest point from the impulse response, and considered only the neighboring impulses in the specified window, forcing the other values to zero. If the window is designed correctly, the dominant impulses will remain, and the channel estimation will not lose accuracy. However, a poorly specified window can yield equally poor channel estimates. The results are shown in Figs. 3(b) and 3(d). In our experiment, we used a window of size 10 samples. This way, the spurious peaks were removed from the estimated channel transfer function, which became smoother. It can also be noted from Fig. 3(b) that the amplitude response of the channel remained stable between the first and last pilots stored for offline processing (10 μs time interval).

We also evaluated the difference in performance between zero-forcing and MMSE equalizers. The design of a proper MMSE equalizer requires knowledge of the received signal SNR, as indicated in Eq. (3). Since in the experimental setup it is relatively difficult to estimate the precise noise variance, we varied the SNR over a wide range and calculated the bit error rate for each case. The results are shown in Fig. 4. It can be seen that, for all investigated transmission rates, the BER is minimized when the assumed SNR^{-1} is equal to zero, effectively turning the MMSE equalizer into a zero-forcing equalizer. Therefore, we expect both equalizers to exhibit similar performances. This conclusion is consistent with the results obtained by [15].

We considered transmission rates from 5 to 10 Gbps. Thus, the bit duration is at least $T_b = 100$ ps. As we transmitted the SC-FDE signal over an OM3 fiber of 2443 m, with 3300 MHz \times km bandwidth, the channel duration is around 740 ps, or approximately 8 bits, at 10 Gbps, and 4 bits at 5 Gbps. Hence, the minimum size of the cyclic prefix is 8 bits in order to avoid interblock interference at the worst case of a transmission rate of 10 Gbps. For short blocks, this required overhead can become excessively large. For this reason, we choose to transmit SC-FDE blocks of size 1024 bits. Therefore, the overhead caused by the cyclic prefix

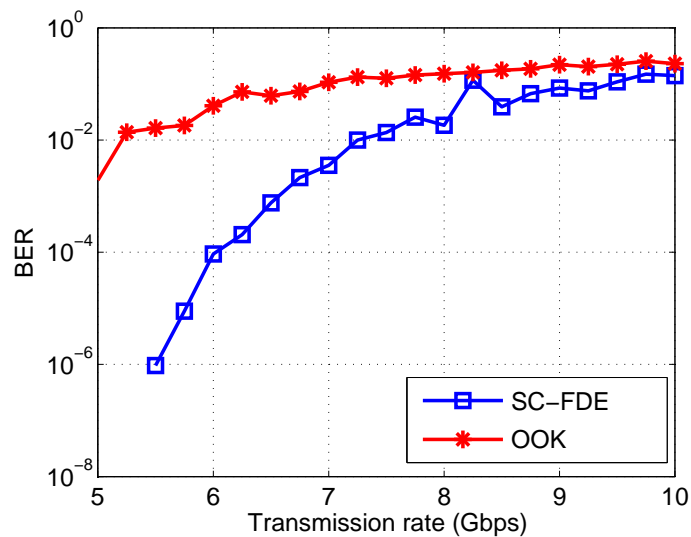


Fig. 5. Bit error rate versus transmission rate for the zero-forcing equalizer. The received signal power was kept constant at -9 dBm.

addition does not become significant. Also, the block does not become so long as to require a high capacity buffering at the receiver. To compare the performance of SC-FDE to a simple OOK transmission, we calculated the BER for different transmission rates considering both systems, as seen in Fig. 5. As expected, the SC-FDE system outperformed the OOK in all cases, presenting an error-free transmission (over a 4 Mbit sequence) for transmission rates inferior to 5.5 Gbps. The results show that SC-FDE modulation can improve the performance of current short distance systems, which are mostly based on OOK modulation.

It is important to note that, although error-free transmission has been achieved at a rate of 5 Gbps, the investigated fiber had a length of 2443 m, which is longer than required in most data center applications. Assuming modal dispersion as the dominant bandwidth-limiting effect, we can conjecture that 40 Gbps would be feasible using an OM3 fiber of nearly 300 m (multiplying the bit rate by 8 and dividing the achievable length by the same factor), which is still sufficient for many local area applications. However, other impairments such as chromatic dispersion, modal noise, transmitter and receiver limited bandwidths do not necessarily scale and must also be investigated carefully, particularly at higher rates. Further developments may also include forward error correction in the analysis.

4. Conclusion

In this work we proposed and experimentally demonstrated the use of SC-FDE with OOK modulation for mitigating intermodal dispersion in short-reach optical systems. We were able to obtain error-free transmission (over a 4 Mbit sequence) for 5 Gbps over 2443 meters of OM3 fiber. Compared with OFDM, SC-FDE simplifies the transmitter avoiding the generation of complicated waveforms, while the total computational complexity is maintained. Therefore, we believe that SC-FDE is a promising alternative to enable cost-effective high-capacity MMF transmission using 850 nm VCSELs, OOK modulation format and direct detection. Future works may also include forward error correction in the analysis.

Acknowledgments

This work was supported by the CPqD Foundation.